BRAF Mutation Status in Gastrointestinal Stromal Tumors

Isabelle Hostein, PhD,[1] Nicolas Faur, MSc,[1] Charlotte Primois,[1] Frédérique Boury,[1] Jérome Denard, MSc,[1] Jean-François Emile, MD,[2] Pierre-Paul Bringuier, MD,[3] Jean-Yves Scoazec, MD,[3] and Jean-Michel Coindre, MD[1]

Key Words: *BRAF*; Gastrointestinal stromal tumors; GIST; Mutations

DOI: 10.1309/AJCPPCKGA2QGBJ1R

Abstract

Gastrointestinal stromal tumors (GISTs) are mesenchymal tumors characterized by mutations of KIT *or* PDGFRA. *The objectives of this study were to evaluate* BRAF *mutations in GISTs and then to correlate* BRAF *mutational status in the tumor with clinical parameters, with B-raf expression, and with activation of some cellular pathways.* BRAF *mutation was screened in 321 GISTs with 70 wild-type GISTs.* BRAF *V600E was detected in 9 (13%) of 70 wild-type GISTs. No mutations were detected in GISTs bearing* KIT *or* PDGFRA *mutations.* BRAF *V600E detection in the tumor does not induce a higher expression of the B-raf protein or the preferential activation of the p42/44 mitogen-activated protein kinase (MAPK) signaling pathway compared with GISTs without the* BRAF *mutation. In comparison with the GIST group with* KIT *or* PDGFRA *mutation or the wild-type GIST group without* BRAF *mutation, the wild-type GIST group with a* BRAF *mutation is not different in terms of B-raf expression or the p44/42 MAPK- or AKT-activated signaling pathway.*

Gastrointestinal stromal tumors (GISTs) are mesenchymal tumors arising in the intestinal tract, mainly in the stomach and the small intestine. They are characterized by mutations in the *KIT* (80%) or the *PDGFRA* gene (8%).[1,2] Nevertheless, approximately 10% to 15% of GISTs are free of *KIT* or *PDGFRA* mutations.[3] The downstream signaling cascade activated by *KIT* includes the Ras-Raf–mitogen-activated protein kinase (MAPK) pathway, the phosphatidylinositol-3-kinase pathway, and the Jak-STAT kinase pathway.[4,5] According to the type of *KIT* mutation, one of these pathways is activated preferentially.[5]

The *BRAF* gene encodes for a serine/threonine-protein kinase.[6] Its function is to control proliferation and differentiation through the Ras-Raf-MAPK pathway. It is mutated in a wide range of cancers, with a high rate in malignant melanoma, thyroid carcinoma, and colorectal cancer with microsatellite instability.[7] Most mutations lie within the kinase domain with a single nucleotide substitution at position 1799 in exon 15, leading to the V600E amino-acid substitution (98%). The remaining 2% are located in exon 11. Germline mutations of *BRAF* have been described in the cardio-facio-cutaneous syndrome within exons 6, 11, 12, and 14.[8,9] Recently, the *BRAF* mutation was detected in 3 GISTs without *KIT* or *PDGFRA* mutation and in 1 tumor after imatinib treatment failure.[10]

Imatinib mesylate is the first drug to target directly the mutated protein responsible for the cancer.[11] It inhibits *KIT*, *PDGFRA*, and BCR-ABL tyrosine kinase in GISTs and chronic myelogenous leukemia. It is also very effective in GISTs bearing the exon 11 *KIT* mutation and in GISTs bearing the exon 9 mutation, but at higher dose.[12] GISTs with *KIT* mutations in exon 13 or 17, with p.Asp842Val mutations in *PDGFRA* or without mutations in *KIT* or *PDGFRA* are more

frequently imatinib-resistant. The challenge is not only to find new drugs able to act on GISTs resistant to the available drugs but also to identify other genomic alterations responsible for this cancer. In this study, we analyzed a series of 321 GISTs for *BRAF* mutations. *BRAF* mutation detection in GISTs would be interesting because therapeutic targets against *BRAF* V600E are under investigation and seem promising.[13,14]

Materials and Methods

Tumors

GISTs were collected from the Department of Pathology, Institut Bergonié (Bordeaux, France). Tumors were collected in agreement with the national ethical committee. The diagnosis of GIST was based on tumor location, histologic aspect, c-KIT and protein kinase C θ immunoreactivity, and molecular analysis. Most of the GISTs reported in this study were immunohistochemically positive for c-KIT, except 13 cases in which *PDGFRA* mutations were identified and 2 cases (with no *KIT* nor *PDGFRA* mutations) positive for protein kinase C θ immunostaining.

For the study, 524 GISTs from Institut Bergonié were analyzed for *KIT* and *PDGFRA* mutations from 2004 to 2008. *KIT* and *PDGFRA* mutations were detected in 86.6% of the cases, approximately 75% and 25%, respectively, whereas GISTs with no *KIT* or *PDGFRA* mutations were detected in 13.4% of the cases (70 cases). Among GISTs bearing a *KIT* or *PDGFRA* mutation and analyzed for *BRAF* mutation (251 tumors), 12 tumors were metastatic; 5 represented relapse, 4 tumors after treatment with imatinib mesylate; 2 were primary tumors after treatment with imatinib mesylate; and others were primary untreated tumors. For GISTs without *KIT* or *PDGFRA* mutations (70 tumors), 3 tumors involved relapse, 2 were metastatic, 2 were primary tumors after treatment, and others were primary untreated tumors. Protein S-100 staining was analyzed for wild-type (WT) GISTs and was negative or focal in all cases.

Morphologic, immunohistologic, and clinical data for GISTs without *KIT* or *PDGFRA* mutations are shown in **Table 1**.

DNA Extraction

For fixed tissues, fifteen to thirty 10-μm sections were cut from the paraffin block, depending on tumor cell density. Sections were scraped off the block, deparaffinized twice in toluene, rinsed twice with absolute ethanol, and washed with TNE (10 mmol/L tris(hydroxymethyl)aminomethane [Tris], 1 mmol/L EDTA, and 100 mmol/L sodium chloride). Tissues were resuspended with 500 μL TNE with added Proteinase K (final concentration, 10 μg in 100 μL of TNE, Promega, Madison, WI) and incubated overnight at 55°C. Finally, DNA was purified through columns (Wizard DNA Clean-up System, Promega), rinsed through minicolumns (Ultrafree-MC30, Millipore SA, Bedford, MA) with TE (Tris, pH 8, 10 mmol/L; EDTA, pH 8, 1 mmol/L), and suspended in 100 μL TE.

For frozen tissues, DNA was extracted from 50 mg of tumor according to standard procedure using phenol-chloroform and DNA precipitation with ethanol. The DNA concentration was measured by UV absorbance at 260 nm.

Polymerase Chain Reaction

Polymerase chain reaction (PCR) amplifications were performed on exons 11 and 15 of the *BRAF* gene using the primer sets *BRAF* 11F (5′-TTT CTG TTT GGC TTG ACT TGA CT-3′) and *BRAF* 11R (5′-GTC ACA ATG TCA CCA CAT TAC ATA CT-3′) for *BRAF* exon 11, *BRAF* 15F (5′-TCA TAA TGC TTG CTC TGA TAG G-3′) and *BRAF* 15R (5′-AGT AAC TCA GCA GCA TCT CAG G-3′) for *BRAF* exon 15. For the studies, 50 ng of DNA was amplified with the following thermal cycling profile: 95°C for 5 minutes; then 45 cycles of 95°C for 30 seconds, 60°C for 1 minute, and 72°C for 1 minute; with a final extension at 72°C for 10 minutes. A temperature cycle was added for PCR products run on denaturing high-pressure liquid chromatography (DHPLC) for heteroduplex formation: 98°C for 10 minutes, 60°C for 30 minutes, and cooling at 4°C.

Denaturing High-Pressure Liquid Chromatography

The WAVE DNA Fragment Analysis System (Transgenomic, Omaha, NE) was used to detect the heteroduplex PCR products. The elution temperature was calculated using WAVEMAKER software (Transgenomic) and was 56.5°C for *BRAF* exon 15 and 55.5°C for *BRAF* exon 11.

Sequence Analysis

Purification of the PCR product was performed using the GFX PCR DNA and gel band purification kit (GE Healthcare Lifesciences, Buckinghamshire, England). Automated cycle sequencing for both strands was performed using the Big Dye Terminator v1.1 Cycle Sequencing Kit (Applied Biosystems, Foster City, CA). Sequencing reactions were carried out on the ABI Prism 310 Genetic Analyzer (Applied Biosystems). Sequences were compared with the normal sequence by using SeqScape v2.5 software (Applied Biosystems).

BRAF V600E Allele-Specific PCR

PCR amplifications were performed on exon 15 of the *BRAF* gene using primer sets of *BRAF* ASF (5′-GGT GAT TTT GGT CTA GCT ACA TA-3′) and *BRAF* ASR (5′-GGC CAA AAA TTT AAT CAG TGG A-3′). For the studies, 50 ng of DNA was amplified with the following thermal cycling profile: 95°C for 5 minutes; then 35 cycles

DOI: 10.1309/AJCPPCKGA2QGBJ1R

Table 1

Morphologic, Immunohistologic, and Clinical Data for Gastrointestinal Stromal Tumors Without *KIT* or *PDGFRA* Mutation

Case No./ Sex/Age (y)	Tumor Size (mm)	Morphologic Features	Location	Mitoses/ 50 HPF	Event	Treatment	Immunohistochemical Results	
							c-KIT	PKC θ
1/F/37	30	Spindle	Small intestine	1	Primary	No	+	+
2/M/51	21	Spindle	Duodenum	ND	Primary	ND	+	ND
3/F/39	ND	Epithelioid	Stomach	3	Primary	No	+	+
4/F/25	20	Spindle + epithelioid	Stomach	6	Primary	No	+	+
5/F/52	27	Spindle	Small intestine	3	Primary	No	+	+
6*/M/53	200	Spindle	Small intestine	6	Primary	No	+	+
7/M/65	25	Spindle	Small intestine	1	Primary	No	+	–
8/F/56	20	Spindle	Duodenum	7	Primary	No	+	+
9/M/78	20	Spindle	Small intestine	1	Primary	No	+	–
10/F/36	ND	Spindle	Stomach	ND	Primary	ND	+	ND
11*/M/38	25	Spindle + epithelioid	Small intestine	5	Primary	No	+	+
12/F/20	20	Spindle + epithelioid	Stomach	10	Primary	No	+	+
13/M/81	20	Spindle	Small intestine	7	Primary	No	+	+
14/M/82	25	Spindle + epithelioid	Small intestine	1	Primary	No	+	+/–
15/M/71	ND	Spindle	Stomach	ND	Primary	No	+	ND
16/M/76	25	Spindle	Small intestine	3	Primary	No	+	+
17/F/64	25	Spindle	Small intestine	100	Primary	No	–	+
18/F/77	25	Spindle	Duodenum	1	Primary	No	+	ND
19/M/61	25	Spindle	Stomach	25	Primary	No	+	+
20/M/82	32	Spindle	Stomach	0	Primary	No	+	+
21/M/33	20	Spindle	Small intestine	15	Primary	No	+	+
22/M/67	20	Spindle	Stomach	1	Primary	No	+	+/–
23/F/82	85	Spindle	Stomach	15	Recurrence	Yes	+	+
24/M/28	ND	Spindle + epithelioid	Stomach	0	Primary	No	+	+
25/M/50	12	Spindle	Small intestine	125	Primary	No	+	+
26/M/73	33	Spindle + epithelioid	Stomach	12	Primary	No	+	+
27*/M/63	ND	Spindle	Stomach	ND	Primary	No	–	+
28*/M/78	30	Spindle	Stomach	1	Primary	No	+	–
29/F/58	30	Spindle	Stomach	4	Primary	No	+	ND
30/M/68	18	Spindle	Small intestine	1	Primary	No	+	ND
31/F/69	17	Spindle	Stomach	100	Primary	No	+	ND
32/F/50	30	Spindle	Small intestine	5	Primary	No	+	ND
33*/F/51	25	Spindle	Small intestine	10	Primary	No	+	ND
34/F/52	210	Spindle	Colon	8	Recurrence	Yes	+	ND
35/F/92	25	Epithelioid	Small intestine	ND	Primary	No	+	ND
36/M/67	20	Epithelioid	Stomach	10	Primary	No	+	+
37/M/20	28	Spindle	Stomach	10	Primary	No	+	ND
38/M/50	20	Spindle	Peritoneum	15	Primary	Yes	+	ND
39/M/50	10	Spindle + epithelioid	Peritoneum	10	Primary	No	+	ND
40/M/48	30	Epithelioid	Small intestine	50	Primary	No	+	ND
41/M/69	35	Spindle	Peritoneum	3	Primary	No	+	ND
42*/M/58	25	Spindle + epithelioid	Duodenum	1	Primary	No	+	+/–
43/M/77	25	Spindle	Small intestine	25	Primary	No	+	ND
44/F/71	25	Spindle	Small intestine	1	Primary	No	+	ND
45/F/23	ND	ND	Liver	ND	Metastasis	No	+	ND
46/F/80	35	Epithelioid	Stomach	12	Primary	No	+	ND
47*/M/58	25	Spindle	Small intestine	6	Primary	Yes	+	+
48/M/85	ND	Spindle	Colon	ND	Primary	No	+	ND
49/M/39	20	Epithelioid	Liver	30	Metastasis	ND	+	ND
50/F/42	25	Spindle	Colon	100	Primary	No	+	ND
51/M/46	27	Epithelioid	Stomach	30	Primary	No	+	+
52/F/66	25	Epithelioid	Stomach	3	Primary	No	+	ND
53/F/34	30	Spindle	Stomach	250	Primary	No	+	ND
54/F/75	25	Spindle	Stomach	9	Primary	No	+	+
55*/M/41	25	Spindle	Small intestine	3	Primary	No	+	ND
56/M/58	30	Spindle	Small intestine	1	Primary	No	+	–
57/F/61	ND	Spindle	Stomach	ND	Primary	No	+	ND
58/F/67	120	Spindle	Peritoneum	17	Recurrence	No	+	+
59/M/62	75	Spindle	Stomach	38	Primary	No	ND	ND
60/M/68	25	Spindle	Duodenum	250	Primary	No	+	+
61/M/79	30	Spindle + epithelioid	Small intestine	3	Primary	No	+	ND
62/F/11	15	Spindle + epithelioid	Stomach	30	Primary	No	+	+
63/F/20	ND	Spindle	Stomach	20	Primary	No	ND	ND
64*/F/50	28	Epithelioid	Peritoneum	50	Primary	No	+	ND
65/M/61	25	Epithelioid	Stomach	3	Primary	No	+	ND
66/F/62	ND	Spindle	Stomach	100	Primary	No	ND	ND
67/F/66	ND	Spindle	Rectum	45	Primary	No	ND	ND
68/F/71	30	Epithelioid	Stomach	6	Primary	No	+	ND
69/F/83	ND	Spindle	Small intestine	0	Primary	No	+	+
70/M/85	30	Spindle	ND	1	Primary	No	+	+/–

HPF, high-power fields; ND, not determined; PKC, protein kinase C; +, positive staining; +/– weak staining; –, no staining.
* Cases with the *BRAF* V600E mutation.

DOI: 10.1309/AJCPPCKGA2QGBJ1R

of 95°C for 30 seconds, 60°C for 1 minute, and 72°C for 1 minute; with a final extension at 72°C for 10 minutes. The reliability of the results was determined for each experiment using a positive control sample (DNA extracted from a papillary carcinoma of the thyroid positive for the *BRAF* V600E mutation). Moreover, each sample was previously amplified for *BRAF* exon 15 as described, to ensure that it was possible to obtain a PCR product with a similar size.

B-raf Immunohistochemical Analysis

Immunostaining

First, 4-µm-thick paraffin sections were cut and mounted on glass slides (SuperFrost+, Menzel-Gläser, Braunschweig, Germany). Preparations were dried for 1 hour at 58°C and then overnight at 37°C. Sections were deparaffinized with toluene and rehydrated with ethanol. Preparations were preheated, and a heat-based antigen-retrieval method was used before incubation. Endogenous peroxidase was blocked using a 3% hydrogen peroxidase solution for 5 minutes. All slides were immunostained for B-raf (monoclonal F-7, Santa Cruz Biotechnology, Santa Cruz, CA) at a dilution of 1:50. Sections were incubated for 1 hour at room temperature with the primary antibodies followed by staining with a streptavidin-biotin peroxidase kit (Chem-Mate detection kit/DAB, DakoCytomation, Glostrup, Denmark). Sections were then revealed in a diaminobenzidine solution for 15 minutes and stained with hematoxylin for 1 minute.

Western Blot

For Western blotting, 50 mg of tumor was prepared by grinding in the following: a RIPA buffer (Sigma-Aldrich, St Louis, MO) with phosphatase inhibitors (sodium fluoride, 30 mmol/L; β-glycerophosphate, 40 mmol/L; sodium pyrophosphate, 20 mmol/L; and sodium orthovanadate, 1 mmol/L) and with some protease inhibitors (PIC, Sigma). Equivalent amounts of protein (50 µg) from clarified lysates were resolved with sodium dodecyl sulfate–polyacrylamide gel electrophoresis, transferred to polyvinylidene fluoride membranes, and immunoblotted sequentially with the following antibodies: anti-panAKT (clone 11E7, dilution 1/1,000; Cell Signaling Technology, Danvers, MA), anti–p44/42 MAPK (clone 137F5, dilution 1/1,000; Cell Signaling Technology), anti-AKT (clone 11E7, dilution 1/1,000; Cell Signaling Technology) and anti-phospho-AKT (clone 193H12, dilution 1/1,000; Cell Signaling Technology), anti–phospho-p44/42 MAPK (clone 20G11, dilution 1/1,000; Cell Signaling Technology), and anti-β-actin (dilution 1/10,000; Cell Signaling Technology). After washes, membranes were probed with antirabbit immunoglobulin–horseradish peroxidase conjugate and incubated with Amersham ECL Plus substrate (GE Healthcare Lifesciences).

Results

BRAF Mutation Detection

Among the 454 GISTs bearing *KIT* or *PDGFRA*, 251 were analyzed for *BRAF* mutation by DHPLC, sequencing, and/or V600E-allele specific PCR, and no V600E mutation was detected. Three polymorphisms were detected in 2 tumors in intron 14 as c.IVS14-32G>A and c.IVS14-39G>A in one tumor and IVS14-37G>A in the other; owing to localization in the intron, the polymorphisms do not likely induce abnormal splicing. A similar polymorphism has been previously reported.[15]

We screened 70 GISTs without *KIT* or *PDGFRA* mutation for the *BRAF* mutation by DHPLC, direct sequencing, and V600E allele-specific PCR. Nine cases were positive for V600E mutation, and no other mutations were detected in exon 15 of *BRAF*. The V600E mutation was only detected by allele-specific PCR for 2 cases. All cases with *BRAF* mutations were primary tumors. The *KIT* and *PDGFRA* mutation detection analysis in GISTs is based on prescreening by DHPLC. Nevertheless, the absence of mutation in the WT GISTs has been confirmed by direct sequencing of *KIT* (exons 9, 11, 13, and 17) and *PDGFRA* (exons 12, 14, and 18).

The *BRAF* exon 11 mutation was screened by direct sequencing in 85 GISTs with a *KIT* or *PDGFRA* mutation and in 40 WT GISTs. No mutation was detected, but 2 polymorphisms (p.Arg444Arg) were detected in the WT GIST group.

Clinical Parameters

GISTs with *BRAF* mutations were mainly localized in the small intestine (5/9 [56%]) but also in the stomach (2/9 [22%]) **Table 2**. There was statistically no difference in tumor location between WT GISTs with or without *BRAF* mutations (Fisher exact test). Other histologic and clinical parameters (age, mitoses/50 high-power fields, and tumor size) between the 2 groups were statistically similar (Student

Table 2
Tumor Location According to the *BRAF* Mutational Status in Gastrointestinal Stromal Tumors Without *KIT* or *PDGFRA* Mutation

Tumor Location	No. (%) of Tumors	
	Wild Type for *BRAF* (n = 57)	With *BRAF* Mutation (n = 9)
Small intestine	19 (33)	5 (56)
Stomach	26 (46)	2 (22)
Colon	3 (5)	0 (0)
Rectum	1 (2)	0 (0)
Duodenum	4 (7)	1 (11)
Peritoneum	4 (7)	1 (11)

DOI: 10.1309/AJCPPCKGA2QGBJ1R

Table 3
Clinicopathologic Data Comparison Between Wild-Type *BRAF* and *BRAF* Mutant Gastrointestinal Stromal Tumors Without *KIT* or *PDGFRA* Mutation

	No *BRAF* Mutation		V600E *BRAF* Mutation	
	No. of Cases	**Mean (Range)/Median**	**No. of Cases**	**Mean (Range)/Median**
Mitotic count (/HPF)	54	26 (0-250)/7	8	10 (1-50)/5.5
Tumor size (mm)	50	32 (10-210)/25	8	48 (25-200)/25
Age (y)	61	59 (11-92)/62	9	53 (38-78)/52

HPF, high-power fields.

t test) **Table 3**. Three patients with *BRAF* mutations had a high risk of malignancy (cases 6, 33, and 64), 3 had intermediate risk (cases 11, 42, and 47), and 2 had low risk (cases 28 and 55). For the last patient (case 27), the size of the tumor and the number of mitoses for 50 high-power fields were not determined.

B-raf Expression in GIST

B-raf expression was studied in a total of 37 GISTs. Eight tumors were WT GISTs with *BRAF* V600E mutations, 9 cases were WT GISTs without *BRAF* mutations, and 20 cases were GISTs with *KIT* or *PDGFRA* mutations. The localization of the staining was cytoplasmic **Image 1**. The immunohistochemical results for B-raf detection in GISTs are summarized in **Table 4**. B-raf expression was observed in all cases examined. The intensity of the staining varied from moderate to high, whatever the *KIT*, *PDGFRA*, or *BRAF* mutational status. In the majority of cases, more than 80% of the tumor cells expressed B-raf. No difference for B-raf expression detected by immunohistochemical analysis was observed between the different groups of tumors according to *KIT* or *PDGFRA* and *BRAF* mutational status.

Cellular Signaling Pathway Activation

Activation of the p44/42 MAPK and AKT pathways was investigated in GISTs bearing V600E *BRAF* mutations in comparison with other GISTs **Image 2**. Only 1 frozen tumor with a *BRAF* mutation was available. Frozen tumor was also available for 2 GISTs without *KIT* or *PDGFRA* mutation, 2 GISTs with *PDGFRA* mutations, and 3 with *KIT* mutations. The p44/42 MAPK signaling pathway was activated in all cases, and the intensity of the signal for MAPK and phosphorylated MAPK was similar in all cases, except for phosphorylated MAPK in a case of WT GIST without a *BRAF* mutation. The AKT signaling pathway was similar in all cases except 2 GISTs with *PDGFRA* mutations in which the signal for phosphorylated AKT was higher than in the other cases. Nevertheless, the AKT signaling pathway in the case with a *BRAF* V600E mutation was similar to the WT GIST and GISTs with *KIT* mutations.

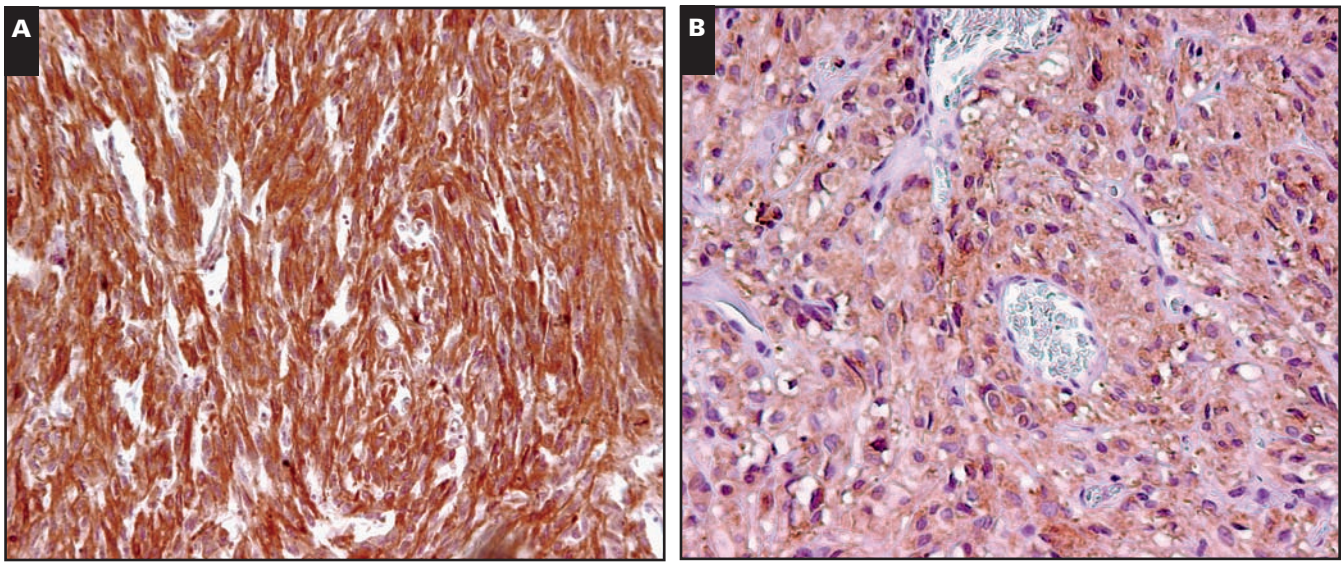

Image 1 B-raf expression in a gastrointestinal stromal tumor. **A** (Case 6, Table 4), Intense cytoplasmic staining in the tumor cells (×200). **B** (Case 11, Table 4), Moderate cytoplasmic staining (×200).

DOI: 10.1309/AJCPPCKGA2QGBJ1R

Table 4
Immunohistologic Analysis for B-raf Expression in Gastrointestinal Stromal Tumors

Patient No.	Staining Intensity*	Tumoral Cells With B-raf Expression (%)	*BRAF* V600E Mutation	*KIT* or *PDGFRA* Mutation
3	2+	80	No	No
6	3+	100	Yes	No
8	2+	100	No	No
33	2+	50	Yes	No
11	1+	90	Yes	No
38	3+	90	No	No
39	1+	90	No	No
42	2+	80	Yes	No
43	3+	90	No	No
19	2+	80	No	No
47	3+	100	Yes	No
22	2+	70	No	No
23	3+	100	No	No
55	2+	90	Yes	No
56	2+	100	No	No
27	2+	90	Yes	No
28	1+	40	Yes	No
71	1+	90	No	*PDGFRA* exon 18
72	3+	90	No	*KIT* exon 11
73	3+	90	No	*KIT* exon 9
74	2+	90	No	*KIT* exon 11
75	2+	100	No	*KIT* exon 11
76	2+	90	No	*PDGFRA* exon 18
77	1+	80	No	*KIT* exon 11
78	2+	80	No	*KIT* exon 11
79	2+	70	No	*KIT* exon 9
80	3+	80	No	*KIT* exon 11
81	1+	60	No	*KIT* exon 11
82	1+	80	No	*KIT* exon 11
83	1+	90	No	*PDGFRA* exon 18
84	1+	80	No	*KIT* exon 11
85	–	—	No	*PDGFRA* exon 18
86	–	—	No	*PDGFRA* exon 18
87	2+	100	No	*KIT* exon 11
88	1+	90	No	*PDGFRA* exon 18
89	3+	100	No	*KIT* exon 11
90	3+	100	No	*KIT* exons 11 and 17

* –, negative; 1+, moderate; 2+, intermediate; 3+, high.

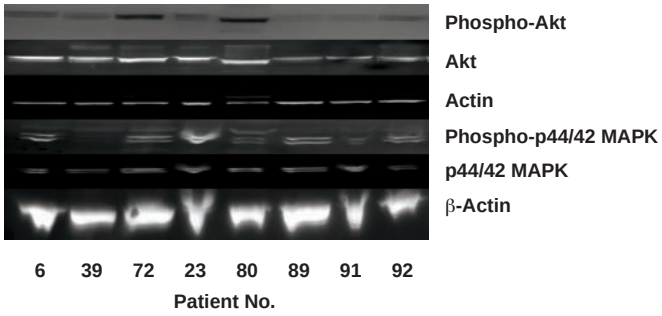

Image 2 Phospho-p44/42 MAPK and phospho-Akt expression in gastrointestinal stromal tumor (GIST) according to *BRAF*, *KIT,* and *PDGFRA* mutational status. No difference in phospho-p44/42 MAPK or phospho-AKT expression was observed according to *BRAF* mutational status. The p44/42 MAPK pathway is not strongly activated in response to a *BRAF* V600E mutation presence in the GIST. Findings for specific cases (from Table 4) were as follows: case 6, wild type, *BRAF* V600E; cases 23 and 39, wild type; cases 72 and 80, *PDGFRA*; and cases 89, 91, and 92, *KIT*.

Discussion

BRAF mutations have been found in a wide range of tumors, but at different levels.[7] They are mainly found in melanoma (60%), thyroid papillary carcinoma (40%), and colorectal tumors with microsatellite instability (10%). *BRAF* is a serine-threonine kinase that activates the MAPK cascade. Mutations of the *BRAF* gene are mainly localized at exon 15 (nucleotide 1799), replacing a valine at position 600 with an aspartic acid. This modification mimics the phosphorylation of the kinase activation domain leading to permanent activation of the kinase. Recently, *KIT* mutations were detected in melanoma at a low percentage (2%).[16] Some of these mutations (eg, p.L576P) have also been detected in GISTs. *KIT* and *BRAF* mutations seem to be exclusive, although Curtin et al[17] described a tumor with the *BRAF* V600E and *KIT* K642E mutations. It cannot be ruled out that the *KIT* K642E mutation is germline because it has been detected in a French family.[18]

Recently, Agaram et al[10] identified *BRAF* mutations in 4% of GISTs without *KIT* or *PDGFRA* mutations and in 1 case of relapse after imatinib treatment. We analyzed *BRAF* mutations in a series of 321 GISTs (70 tumors with no *KIT* or *PDGFRA* mutation and 251 tumors with a *KIT* or *PDGFRA* mutation). The *BRAF* mutation was detected in 9 (13%) of 70 WT GISTs (69 adult and 1 pediatric GIST), and all were the V600E mutation, but was not detected in GISTs with a *KIT* or *PDGFRA* mutation. This percentage is higher than previously described.[10] Excluding GISTs in children in the study by Agaram et al,[10] the frequency of *BRAF* mutants in adults with GISTs was 7% (3/46 cases). In our series, by excluding the pediatric GIST case (case 62), the frequency of *BRAF* mutation is 13% (9/69 cases), twice that described by Agaram et al.[10]

Moreover, for 2 cases in which the percentage of tumor cells was more than 80%, the *BRAF* V600E mutation was probably present in a low percentage of tumor cells because it was detected only by allele-specific PCR, and the sensitivity has been evaluated to be 1% in our hands. The sensitivity of the technique was evaluated by successive dilutions of the colorectal carcinoma cell line HT29 (bearing the p.Val600Glu mutation) in the colorectal carcinoma HCT15 cell line that does not bear this mutation (data not shown). This observation suggests that some subsets of cells gain this specific genetic alteration in the tumor with consequences that remain to be determined. In the thyroid, the *BRAF*

DOI: 10.1309/AJCPPCKGA2QGBJ1R

mutation has been correlated with aggressive pathologic data such as lymph node metastasis, extrathyroidal invasion,[19] worse outcome,[20] and recurrence. In melanoma, the *BRAF* mutation has been associated with increased tumor cell proliferation and shorter survival.[21,22] A larger cohort of WT GISTs with clinical follow-up should be studied for *BRAF* mutations to evaluate the prognostic significance of this mutation.

It seems that *KIT* and *BRAF* mutations are exclusive as in melanoma tumors because of 251 GISTs with a *KIT* or *PDGFRA* mutation, no *BRAF* mutations for exon 15 or 11 were detected.

The significance of *BRAF* mutations in GISTs negative for *KIT* or *PDGFRA* mutation is unknown, although there should be a biologic impact in the tumor because this mutation has been selected during tumor development. BRAF is an important protein that interacts with ras to transduce a signal through the MAPK pathway,[6] a signaling pathway that is activated in GISTs. In evaluating the activation of the MAPK and AKT pathways, no difference was observed between WT GISTs with the V600E mutation (although only 1 WT GIST with a V600E mutation was available as frozen material) and other WT GISTs or GISTs with a *KIT* or *PDGFRA* mutation. Although a *BRAF* mutation is detected, it does not seem to preferentially activate the MAPK pathways. The same observation has been made in melanoma[23] and in thyroid; 170 melanomas[24] and 42 papillary carcinomas[25] were screened for *BRAF* mutations and compared with MAPK activation pathways by immunohistochemical analysis. No obvious relation between *BRAF* mutational status and MAPK activation has been found. We have also investigated B-raf immunostaining in WT GISTs with or without *BRAF* mutations and in GISTs with a KIT or *PDGFRA* mutation (Table 4). Whatever the mutational status of the tumor, no significant difference in the percentage of tumor cells stained or the intensity of the staining was observed. The same observation was made in thyroid carcinoma.[26]

As reported by Agaram et al,[10] we observed a predominant small intestinal location of GISTs with *BRAF* V600E (56%) followed by location in the stomach (22%). Nevertheless, the repartition of tumor localization is similar to that reported for GISTs.[27] No clinicopathologic data such as tumor size, mitotic count, or age seem to be specific to GISTs bearing V600E *BRAF* mutations. Unfortunately, we were not able to learn the clinical follow-up for these patients.

We report *BRAF* mutation status in GISTs without a *KIT* or *PDGFRA* mutation. The level of mutation affects 13% of GISTs without a *KIT* or *PDGFRA* mutation. This observation may be very important because there is as yet no treatment for this set of GISTs. Although this observation as been reported previously, we observed a higher V600E detection rate in this subset of tumors. Although the preferential location to the small intestine for this group of tumors is not statistically relevant, it confirms what was observed by Agaram et al.[10] A drug targeting *BRAF* is being tested in phase 1 and 2 trials in melanoma[28] and renal carcinoma[29] and might also be effective in *BRAF*-mutated GISTs. Further studies are needed to evaluate more precisely the incidence of *BRAF* mutations in the WT GIST subset and to investigate the function of the mutation in GISTs.

From the [1]Department of Pathology, Institut Bergonié, Bordeaux; [2]Assistance Publique-Hôpitaux de Paris, Ambroise Pare Hospital, Boulogne; and [3]Department of Pathology, Edouard Herriot Hospital, Lyon, France.

Supported by CONTICANET (Connective Tissue Cancers Network to Integrate European Experience in Adults and Children), Lyon, France.

Address reprint requests to Dr Hostein: Dept of Pathology, Institut Bergonié, 229 cours de l'Argonne 33076 Bordeaux cedex, France.

References

1. Gomes AL, Bardales RH, Milanezi F, et al. Molecular analysis of c-KIT and PDGFR in GISTs diagnosed by EUS. *Am J Clin Pathol*. 2007;127:89-96.
2. Heinrich MC, Corless CL, Duensing A, et al. PDGFR activating mutations in gastrointestinal stromal tumors. *Science*. 2003;299:708-710.
3. Steigen SE, Eide TJ, Wasag B, et al. Mutations in gastrointestinal stromal tumors: a population-based study from northern Norway. *APMIS*. 2007;115:289-298.
4. Duensing A, Medeiros F, McConarty B, et al. Mechanisms of oncogenic KIT signal transduction in primary gastrointestinal stromal tumors (GISTs). *Oncogene*. 2004;13:3999-4006.
5. Casteran N, De Sepulveda P, Beslu N, et al. Signal transduction by several KIT juxtamembrane domain mutations. *Oncogene*. 2003;22:4710-4722.
6. Schreck R, Rapp UR. Raf kinases: oncogenesis and drug discovery. *Int J Cancer*. 2006;119:2261-2271.
7. Davies H, Bignell GR, Cox C. Mutations of the *BRAF* gene in human cancer. *Nature*. 2002;417:949-954.
8. Niihori T, Aoki Y, Narumi Y, et al. Germline *KRAS* and *BRAF* mutations in cardio-facio-cutaneous syndrome. *Nat Genet*. 2006;38:294-296.
9. Rodriguez-Viciani P, Tetsu O, Tidyman WE, et al. Germline mutations in genes within the MAPK pathway cause cardio-facio-cutaneous syndrome. *Science*. 2006;311:1287-1290.
10. Agaram NP, Wong GC, Guo T, et al. Novel V600E *BRAF* mutations in imatinib-naive and imatinib-resistant gastrointestinal stromal tumors. *Genes Chromosomes Cancer*. 2008;47:853-859.
11. Dagher R, Cohen M, William G, et al. Approval summary: imatinib mesylate in the treatment of metastatic and/or unresectable malignant gastrointestinal stromal tumors. *Clin Cancer Res*. 2002;8:3034-3038.
12. De Giogi U. *KIT* mutations and imatinib dose effects in patients with gastrointestinal stromal tumors [letter]. *J Clin Oncol*. 2007;25:1146-1147.

DOI: 10.1309/AJCPPCKGA2QGBJ1R

13. Hoeflich KP, Herter S, Tien J, et al. Antitumor efficacy of the novel REF inhibitor GDC-0879 is predicted by $BRAF^{V600E}$ mutational status and sustained extracellular signal-regulated kinase/mitogen-activated protein kinase pathway suppression. *Cancer Res*. 2009;69:3042-3051.
14. Tsai J, Lee JT, Wang W, et al. Discovery of a selective inhibitor of oncogenic B-Raf kinase with potent antimelanoma activity. *Proc Natl Acad Sci U S A*. 2008;105:3041-3046.
15. James MR, Dumeni T, Stark MS, et al. Rapid screening of 4000 individuals for germ-line variations in the *BRAF* gene. *Clin Chem*. 2006;52:1675-1678.
16. Wilmore-Payne BS, Holden JA, Tripp S, et al. Human malignant melanoma: detection of *BRAF* and c-*KIT* activating mutations by high-resolution amplicon melting analysis. *Hum Pathol*. 2005;36:486-493.
17. Curtin JA, Busam K, Pinkel D, et al. Somatic activation of KIT in distinct subtypes of melanoma. *J Clin Oncol*. 2006;24:4340-4348.
18. Graham J, Debiec-Rychter M, Corless LC, et al. Imatinib in the management of multiple gastrointestinal stromal tumors associated with a germline *KIT* K642E mutation. *Arch Pathol Lab Med*. 2007;131:1393-1396.
19. Oler G, Carnacho CP, Hojaij FC, et al. Gene expression profiling of papillary thyroid carcinoma identifies transcripts correlated with *BRAF* mutational status and lymph node metastasis. *Clin Cancer Res*. 2008;14:4735-4742.
20. Elisei R, Ugolini C, Viola D, et al. *BRAF* V600E mutation and outcome of patients with papillary thyroid carcinoma: a 15-year median follow-up study. *J Clin Endocrinol Metab*. 2008;93:3943-3949.
21. Johansson P, Pawey S, Hayward N. Confirmation of a BRAF mutation-associated gene expression signature in melanoma. *Pigment Cell Res*. 2007;20:216-221.
22. Hoeflich KP, Gray DC, Eby MT, et al. Oncogenic *BRAF* is required for tumor growth and maintenance in melanoma models. *Cancer Res*. 2006;66:999-1006.
23. Houben R, Vetter-Kauczok CS, Ortmann S, et al. Phospho-ERK staining is a poor indicator of the mutational status of *BRAF* and *NRAS* in human melanoma. *J Invest Dermatol*. 2008;128:2003-2012.
24. Venesio T, Chiorino G, Balsamo A, et al. In melanocytic lesions the fraction of *BRAF* V600E alleles is associated with sun exposure but unrelated to ERK phosphorylation. *Mod Pathol*. 2008;21:716-726.
25. Zuo H, Yasuoka H, Zhang P, et al. Lack of association between *BRAF* V600E mutation and mitogen-activated protein kinase activation in papillary thyroid carcinoma. *Pathol Int*. 2007;57:12-20.
26. Kondo T, Nakazawa T, Murata SI, et al. Enhanced B-Raf protein expression is independent of V600E mutant status in thyroid carcinomas. *Hum Pathol*. 2007;38:1810-1818.
27. Biasco G, Velo D, Angriman I, et al. Gastrointestinal stromal tumors: report of an audit and review of the literature. *Eur J Cancer Prev*. 2009;18:106-116.
28. Eisen T, Ahmad T, Flaherty KT, et al. Sorafenib in advanced melanoma: a phase II randomized discontinuation trial analysis. *Br J Cancer*. 2006;95:581-586.
29. Ahmad T, Eisen T. Kinase inhibition with BAY 43-9006 in renal cell carcinoma. *Clin Cancer Res*. 2004;10(18 pt 2):6388S-6392S.

DOI: 10.1309/AJCPPCKGA2QGBJ1R

HOLOGIC®

First and Only FDA Cleared
Digital Cytology System

Genius™ Cervical AI

Genius™ Review Station

Genius™ Digital Imager

Empower Your Genius With Ours

Make a Greater Impact on Cervical Cancer
with the Advanced Technology of the
Genius™ Digital Diagnostics System

Click or Scan
to discover more

genius™
DIGITAL DIAGNOSTICS